New data from borehole strainmeters to infer lava fountain sources (Etna 2011–2012)

A. Bonaccorso,[1] G. Currenti,[1] A. Linde,[2] and S. Sacks[2]

Received 23 April 2013; revised 21 June 2013; accepted 21 June 2013.

[1] In January 2011, eruptive activity resumed at Etna producing a new phase with frequent lava fountain episodes until April 2012. In November 2011, the first two borehole strainmeters were installed, which detected negative strain changes (~0.15–0.8 μstrain) during the paroxysmal events. A Finite Element Model was set up to estimate accurately the tilt and volumetric strain, taking into account the real profile of the volcano and the elastic medium heterogeneity. The numerical computations indicated an elongated depressurizing source located at 0 km b.s.l., which underwent a volume change of ~2 × 10^6 m^3 which is the most of the magma volume erupted, while a smaller remaining part is accommodated by the magma compressibility. This shallow source cannot accumulate large magma volumes and, thus, favors short-term periodic eruptive events with a fairly constant balance between the refilling and the erupted magma. **Citation:** Bonaccorso, A., G. Currenti, A. Linde, and S. Sacks (2013), New data from borehole strainmeters to infer lava fountain sources (Etna 2011–2012), *Geophys. Res. Lett.*, *40*, doi:10.1002/grl.50692.

1. Introduction

[2] Lava fountains are spectacular eruptive phenomena giving rise to powerful and sustained gas jets that expel lava fragments to heights from tens to hundreds of meters [e.g., *Wolff and Sumner*, 2000 and references therein]. These eruptive episodes occur in basaltic volcanoes and, despite their short duration (from minutes to some hours), are an important signature of volcano recharging phases, representing a possible prelude to bigger effusive eruptions. At Etna volcano, during recharging phases preceding the several flank eruptions occurring in recent decades, tens of spectacular lava fountains have taken place [e.g., *Harris and Neri*, 2002; *Behncke and Neri*, 2003; *Allard et al*., 2005]. This paroxysmal activity has often been dramatic because of the formation of a huge eruptive column that, depending on wind intensity and direction, produces ash plume dispersal/ and fall-out deposits. In recent years, this phenomenon has caused problems to the infrastructure of the city of Catania and the other villages around Etna, as well as severe hazard to aviation with frequent temporary closure of the Catania airport. A new series of lava fountains started in January 2011. For these more recent episodes, several studies have been conducted through geochemical and continuously recorded geophysical data [*Aiuppa et al*., 2010; *Calvari et al*., 2011; *Bonaccorso et al*., 2011a; *Bonaccorso et al*., 2011b; *Ganci et al*., 2012]. These recent studies concur in interpreting the lava fountains at Etna as a violent release of a bubble-rich magma layer previously decoupled from the melt and trapped at the top of a shallow reservoir located between −1 and 1.5 km a.s.l. This interpretation would support the "foam collapse model" derived from a combination of theoretical approaches and laboratory experiments [e.g., *Jaupart and Vergniolle*, 1989]. A key open issue is to constrain the source position and its volume change. A first-order estimation of the source depth was obtained through the small tilt changes (~0.2–0.5 microradians) detected by the tiltmeters installed around the volcano flanks [*Bonaccorso et al*., 2011a; 2011b]. At the beginning of November 2011, the first two borehole strainmeters were installed at Etna and detected clear strain changes during lava fountain episodes. *Bonaccorso et al*. (2013) considered two of these episodes and used the relative sensitivities at the two stations to attempt determining a first location of the source using a simple spherical chamber embedded in a homogeneous elastic half-space. In this work, we considered the average strain changes recorded during all the lava fountains and the tilt change constraints. We modeled the data through a more advanced numerical model (finite element method (FEM) approach), taking into consideration both volcano topography and medium heterogeneities to obtain information on source shape, position, and volume change.

2. 2011–2012 Lava Fountain Episodes

[3] After the end of the long-lasting 2008–2009 flank eruption, in January 2011, the eruptive activity resumed at Etna to produce several paroxysmal events from the South-East crater (Figure 1a), one of the four summit craters and the most active in the last years. This eruptive phase continued in 2011 and early 2012, with the last (25^{th}) lava fountain occurring on 24 April 2012. Almost all the lava fountains have the same characteristics with a gradually increasing strombolian phase for a few hours that precedes the paroxystic event. Then, the intensity of explosions increases rapidly, and the activity soon progresses to lava fountains, accompanied by increasing ash emission and lava flow output. In about half an hour, ash emission significantly increases with jets of incandescent bombs reaching ~800 m above the crater and the eruptive column rising several kilometers above the volcano summit (Figure 1b), before being driven to the distal volcano flanks depending on wind direction. The lava fountain episodes are described at www.ct.ingv.it. The paroxysmal episodes last a few hours and fed lava flows that expand in the Valle del Bove depression

[1]Istituto Nazionale di Geofisica e Vulcanologia, Sezione di Catania-Osservatorio Etneo, Catania, Italy.
[2]Department Terrestrial Magnetism-Carnegie Institution, Washington, USA.

Corresponding author: A. Bonaccorso, Istituto Nazionale di Geofisica e Vulcanologia, Sezione di Catania, Piazza Roma, 295123 Catania, Italy. (bonaccorso@ct.ingv.it)

0094-8276/13/10.1002/grl.50692

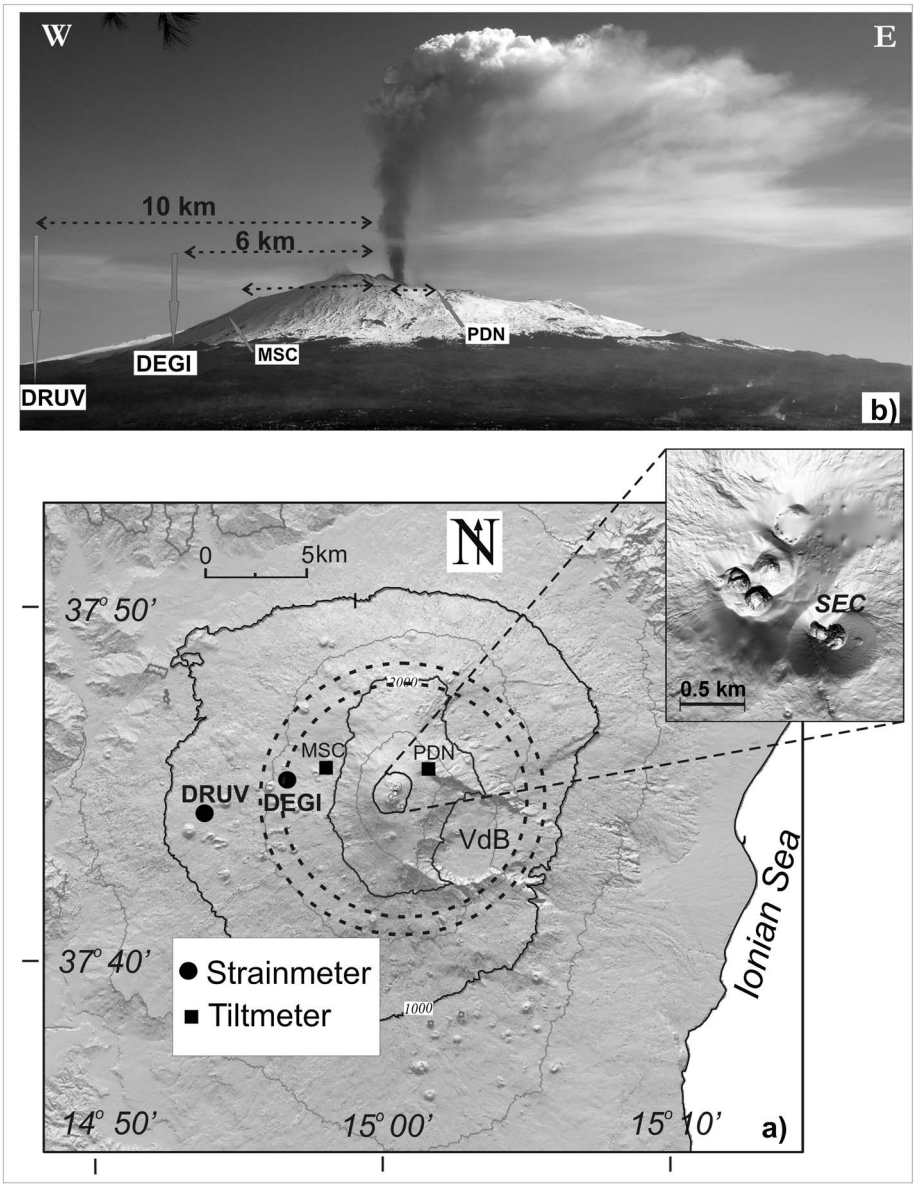

Figure 1. (a) Etna map. The positions of the two borehole strainmeters (DRUV and DEGI) and tiltmeters MSC (~4 km away from central craters) and PDN (~2.2 km from central craters) are indicated. The other eight borehole tiltmeters are installed around the volcano in a circular pattern at almost the same 6–8 km radial distance from summit craters in the area outlined by dotted concentric circles. (b) 18 March 2012 lava fountain. W-E profile of Etna seen from the village of Centuripe (low SW flank). Photo courtesy of D. Condarelli.

(Figure 1) reaching lengths of 5–6 km. Estimates of the volumes of the emitted lava were recently inferred by satellite thermal data [*Ganci et al*., 2012]. The authors analyzed the effusive volume of the 19 lava fountains from 12 January 2011 (first event) to 5 January 2012 (nineteenth event) retrieved from SEVIRI satellite data. In this series, seven events were affected by ash inference and cloudy conditions, and the calculation was not robust. Instead, 12 events were well detected, and they provided a mean effusive volume of 1.75×10^6 m^3. This is the average value representative for the effusive volume of each lava fountain episode. Based on the average value from literature referred to several explosive eruptions at Etna, we assumed that the estimated tephra volume is about 50% of the effusive volume [e.g., *Behncke et al*., 2006; *Andronico et al*., 2008; *Calvari et al*., 2011]. Therefore, the mean total erupted volume that we consider representative during each event was ~2.6×10^6 m^3.

3. Strain Data

[4] A tiltmeter network made up of shallow borehole instruments installed at 3–10 m depth [e.g., *Bonaccorso et al*., 2011a] has been operating at Etna in recent decades. These instruments have a resolution in the order of 10^{-7} radians, and, in case of slow variations (hours to months), the instrumental precision is affected by noise due to temperature and thermoelastic effects [*Bonaccorso et al*., 1999]. One station (MSC in Figure 1) is situated about 4 km from the summit crater area, and the remaining eight borehole stations are installed around the volcano at a near constant radial distance of 6–8 km from summit crater area (Figure 1). The only

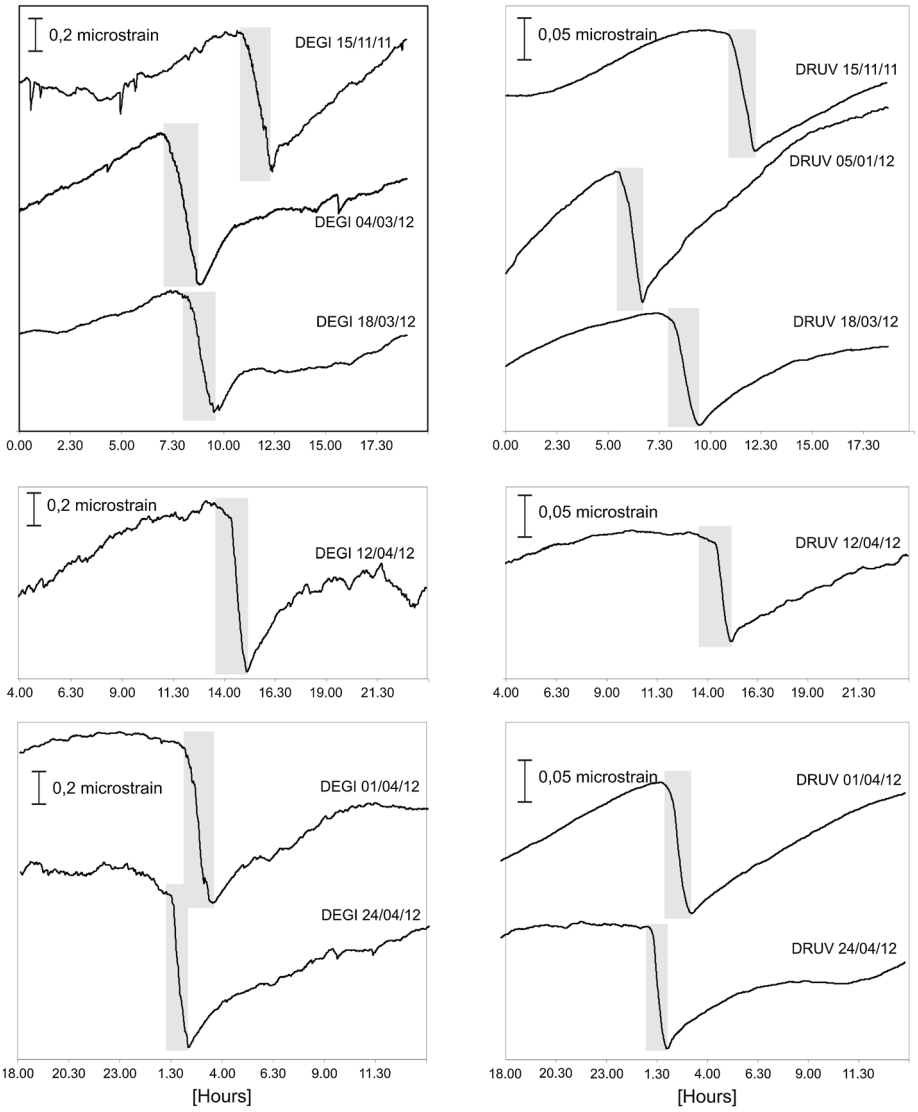

Figure 2. Strain signals recorded at DRUV and DEGI stations showing the negative changes (meaning medium expansion around the sensor) recorded during the lava fountains occurring at Etna from 15 November 2011 to 24 April 2012. For DRUV, the raw data are shown, while for DEGI, due to its drift, the data were detrended using a linear filter.

instrument operating in the summit area, at about 2.2 km from central craters, is a 80 m long-base fluid tiltmeter (PDN in Figure 1) with a slightly better resolution (10^{-7} – 10^{-8} radians) [*Bonaccorso*, 2006]. During the last 2011–2012 phase of lava fountains, the tilt detected small negative changes (indicating deflation) that are difficult to interpret. The PDN summit station recorded 0–0.2 μradians changes, the MSC station about 0.8 – 1.2 μradians, and the remaining stations about 0–0.4 μradians [*Bonaccorso et al*., 2011a, 2011b].

[5] The first two borehole strainmeters were installed at ~180 m depth below the ground surface on the western flank of Etna volcano. The horizontal radial distance from the central crater VOR is ~6 km for DEGI (altitude 1500 m a.s.l.) and ~10 km for DRUV (altitude 1200 m a.s.l.), respectively (Figure 1). These instruments, also known as dilatometers, are Sacks-Everton types and have a resolution of ~10^{-11} [*Sacks et al*., 1971], which enable precise detection of strain changes. A decreasing signal is recorded during expansion and an increasing signal during contraction of the medium surrounding the instrument. After installation procedures, the instruments started to record in the first days of November 2011. Initially, they showed a marked long-term drift, which usually lasts from several months to years [*Roelloffs and Linde*, 2007]. However, the lava fountains represent a fast transient that can be clearly detected even in the presence of a long-term drift. Indeed, the stations recorded significant changes coinciding with all eight lava fountains occurring from 15 November 2011 to 24 April 2012. In order to interpret the data, the measurements require an accurate in situ calibration by relating instrument readings to Earth strains. The calibration factors are determined from the ratios of the observed volumetric strain tide amplitudes to corresponding theoretical strain tide amplitudes. The diurnal Ol (25.82 h) and semidiurnal M2 (12.42 h) lunar tidal components in the strainmeter outputs were estimated using the BAYTAP-G software [*Tamura et al*., 1991]. The raw data records were preprocessed to remove offsets and any outliers. Atmospheric pressure records were also used in the tidal analysis. The theoretical tidal volumetric strain for these components was calculated using the SPOTL package [*Agnew*, 1996], which computes the strains produced by astronomical forces and

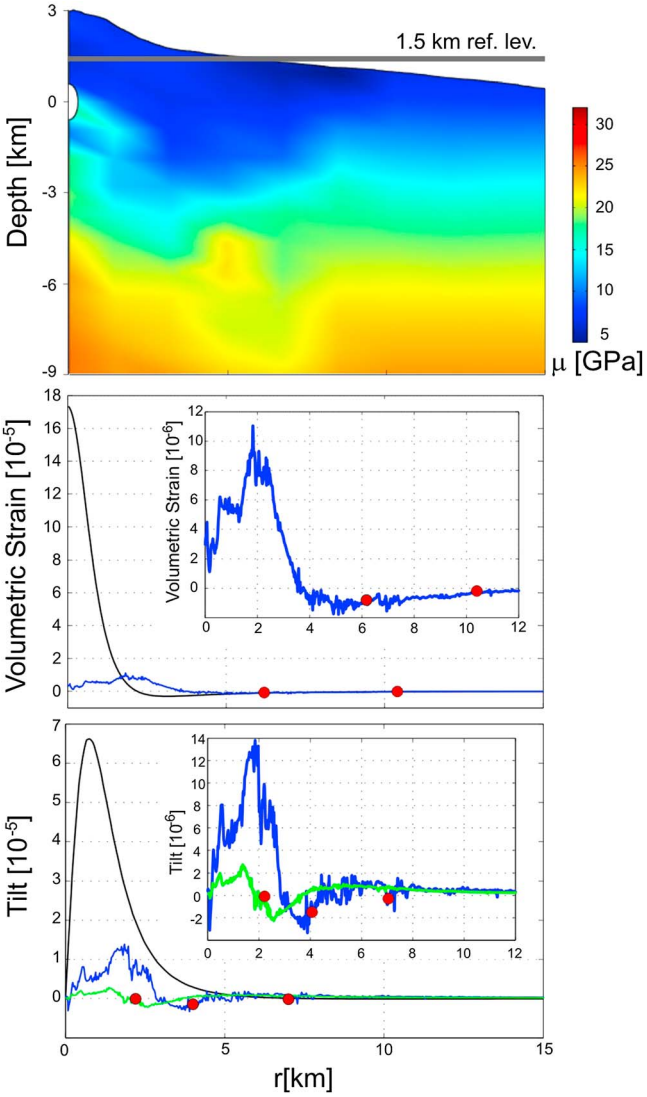

Figure 3. (a) Section of the computational domain of the elastostatic model showing the real topography and elastic medium heterogeneity. The color scale reports the values of rigidity modulus in GPa [*Patanè et al*., 2003]. The reference level of the ground surface for the simple homogeneous half-space (HHS) model is also reported. (b) Computed volumetric strain changes for the HHS (black line) and numerical model (blue line). The average observed strain changes at DRUV and DEGI are shown in circles. (c) Computed tilt for the HHS model (black line) and horizontal (green line) and vertical (blue line) tilts for the numerical model. The representative tilt changes recorded at PDN (2.2 km away from summit craters), MSC (4 km), and other tilt stations (6–8 km) during the lava fountains are also reported as circles. The large discrepancies between the HHS and numerical results in the summit area are mainly due to the topography effect and to the different distance between the observation points and the source depth in the two models. This effect lowers at higher horizontal distances (>3–4 km) where the numerical and HHS results are almost similar.

ocean loading. The calibration factors are obtained by numerically fitting the observed and the theoretical tides, providing a value of 0.005 nstr/counts and 0.01 nstr/counts at DRUV and DEGI, respectively, which means a ratio of 20 between the calibration factors at the two stations. The low coupling coefficient at DEGI with respect to DRUV derives from the lower sensitivity at DEGI, where the instrument is installed in a less massive lava layer. As an independent validation of the computed calibration factors, we compared the surface wave amplitudes from distant, very large earthquakes (M≥8) that for periods shorter than ~30 s showed the DEGI sensitivity to be a factor of 20 less than that of DRUV installed in competent rock [*Bonaccorso et al*., 2013].

[6] In Figure 2, the data collected during the six lava fountains are shown for both DRUV and DEGI signals after the data calibration. All recorded signals showed negative strain changes, indicating medium expansion at both sites. For each fountain episode, the amplitudes of the strain changes were almost similar with 0.15 and 0.8 μstrain at DRUV and DEGI, respectively.

4. Modeling

[7] To constrain the depth and the volume change of the source, we inverted the average strain changes at the two strainmeters and the average tilts recorded at the radial distance of 2.2 km (PDN), 4 km (MSC), and 6–8 km [*Bonaccorso et al*., 2011b; Figure 1], representative of the signal behavior during the lava fountain episodes. The vertical borehole tiltmeters are sensitive primarily to vertical gradients in horizontal displacements, which for small displacement gradients can be approximated as $\partial u_r/\partial z$, where u_r is the radial displacement, and z is the vertical coordinate. On the other hand, the horizontal long-base tiltmeter at PDN is sensitive to the horizontal gradient in the vertical displacements, which can be estimated as $-\partial w/\partial r$, where w is the vertical displacement, and r is the radial coordinate. The horizontal and vertical tilts are generally computed using simple half-space models for which they are equal. However, for a sloping surface, the vertical tilt differs from the horizontal tilt, and topographic effects may significantly affect the estimates of volumetric strain and vertical and horizontal tilts [*Meertens and Wahr*, 1986].

[8] Given the steep topography and elastic medium heterogeneity of Etna volcano, the half-space homogenous assumption is certain to introduce oversimplification into the model and lead to inaccurate estimates. Therefore, using an FEM software [*COMSOL*, 2012], a 3D axial-symmetric elastostatic model was set up to estimate accurately the expected tilt and volumetric strain changes at the stations. The computational domain is nonuniformly meshed with triangular elements, and cubic Lagrangian shape functions are used to ensure a good accuracy in the stress and strain solutions. The mesh resolution is finer near the source (20 m) and becomes coarse at the outer boundaries (2 km). A profile of the real Etna topography derived from a DEM and the elastic medium heterogeneity estimated from seismic tomography were considered (Figure 3). A detailed description of the model set up can be found in *Currenti et al*. [2010]. The profile runs from the western flank to the summit area in order to describe the average slope of Etna volcano, where almost all the stations are located (Figure 1). In this frame, within the FEM model, we computed the elastic deformation and strain fields caused by an ellipsoidal depressurizing source by solving numerically the elastostatic equations. We explored the ranges of the deformation source parameters, namely the depth, aspect ratio, and volume change, in order to match better the observed variations. A

grid search procedure was used varying the depth from 3 km b.s.l. to 1 km a.s.l. with a step of 500 m and aspect ratio from 0.1 to 1.5 with a 0.1 step. For each of these models, the volume change, which best fits the observations, was estimated. We found that a shallow vertical prolate source with an aspect ratio of 0.5 at a depth of 0 km b.s.l., which undergoes a contraction of 2×10^6 m^3, is capable of producing tilt and volumetric strain changes that match the observations reasonably well (Figure 3). The numerical results were also compared with those obtained for the same source embedded in a simple homogeneous half-space (HHS) model with a reference ground surface at 1.5 km a.s.l.

5. Discussion and Conclusions

[9] Due to the topography and the medium heterogeneity of the volcano, the half-space homogenous assumption introduces oversimplification into the source modeling and hence potentially inaccurate estimates in volumetric strain and tilt. Figure 3 clearly shows the marked discrepancy between the HHS and numerical solutions, underlining the important role played by the topography effect. This is particularly critical in the summit area where the steep topography causes large discrepancies in the numerical results with respect to the HHS solutions. However, these discrepancies are much smaller when horizontal distance between observation point and source is greater than 3–4 km (Figure 3). The FEM numerical model satisfies the near-zero horizontal tilt recorded at PDN long-base instrumentation as well as the vertical tilt changes at the other borehole stations; the simple half-space model gives a very much larger tilt. Moreover, the model predicts ground deformation below 1 cm in agreement with the GPS observations from the continuously running stations (M. Mattia personal communication).

[10] The precise strain changes recorded during the lava fountains associated with the FEM approach allowed inferring the position and shape of the source robustly. The numerical computations point to a source at about 0 km b.s.l., which coincides with the position of the seismic tremor source located during the ordinary volcano activity and the lava fountain episodes [e.g., *Bonaccorso et al*., 2011a]. Moreover, the estimated ellipsoid aspect ratio of 0.5 is consistent with the hypothesis of an elongated source simulating the shallow conduit processes. This source represents the shallow storage where bubble-rich magma is trapped and then violently released through lava fountains. The source undergoes a volume change of 2×10^6 m^3, which is slightly less than the average erupted volume for each event of 2.6×10^6 m^3. In general, the difference between the emitted magma volume (ΔV_{magma}) and the volume change of the magma storage source (ΔV_{source}) can be attributed to magma compressibility that under pressure can accommodate a batch of magma ($\Delta V_{compression}$) following this relation:

$$\Delta V_{magma} = \Delta V_{source} + \Delta V_{compression} \quad (1)$$

[11] Following *Johnson et al*. [2000] (1) can be written as:

$$\Delta V_{magma}/\Delta V_{source} = 1 + \frac{3}{4}\mu C \quad (2)$$

where μ is the rigidity modulus of the host rock, and C is the compressibility of magma residing in the source. The ΔV_{magma} is almost equal to ΔV_{source} if the magma is incompressible or if the host medium is very compliant, making the $\Delta V_{compression}$ contribution negligible. Magma compressibility and medium rigidity have a competing behavior in relation to source depth: for deeper sources, the magma compressibility decreases (due to less gas exsolution with depth), and the medium is less compliant since it has a higher rigidity module; on the contrary, the magma compressibility increases while the medium is usually more compliant for shallower sources. Compressibility of basaltic magma is in the range $0.4 - 2 \times 10^{-10}$ Pa^{-1} [*Spera*, 2000] while rigidity in volcanic edifices has a wide range from 0.1×10^9 for shallower compliant rocks to 3×10^{10} Pa for a very stiff medium. This implies that sources located in very compliant crust could produce moderate volume discrepancies between ΔV_{magma} and ΔV_{source}.

[12] Indeed, at Etna, seismic tomography shows a low rigidity modulus (≤10 GPa) in the fractured upper layer (Figure 3), allowing hosting magma volumes in the deformed shallow source and making the ΔV_{magma} comparable to ΔV_{source}. In our case, a mean small volume of magma ($\sim 0.6 \times 10^6$ m^3) was accommodated by compression before each lava fountain event.

[13] Our results provide constraints on magma volumes that may accumulate at shallow depth before being erupted in a region, where short-term magmatic processes, like fractional crystallization and mixing, take place [*Corsaro et al*., 2013]. This source seems incapable of accumulating large magma volumes and shows frequent events with a fairly constant balance between the refilling and the erupted magma.

[14] **Acknowledgments.** AB and GC are indebted to all staff of TecnoLab of the INGV-CT who ensure the regular working of the strainmeters of Etna. We thank an anonymous referee and the Editor A. Newmann for their constructive comments.

References

Agnew, D. C. (1996), SPOTL: Some Programs for Ocean-Tide Loading, SIO Reference Series, 96–8, Scripps Institution of Oceanography.

Aiuppa, A., et al. (2010), Patterns in the recent 2007–2008 activity of Mount Etna volcano investigated by integrated geophysical and geochemical observations, *Geochem. Geophys. Geosyst.*, *11*, Q09008, doi:10.1029/2010GC003168.

Allard, P., M. Burton, and F. Murè (2005), Spectroscopic evidence for lava fountain driven by previously accumulated magmatic gas, *Nature*, *433*, 407–409.

Andronico, D., A. Cristaldi, and S. Scollo (2008), The 4–5 September 2007 lava fountain at South-East Crater of Mt Etna, Italy, *J. Volcanol. Geotherm. Res.*, *173*, 325–328, doi:10.1016/j.jvolgeores.2008.02.004.

Behncke, B., and M. Neri (2003), The July-August 2001 eruption of Mt. Etna (Sicily), *Bull. Volcanol.*, *65*, 461–476, doi:10.1007/s00445-003-0274-1.

Behncke, B., M. Neri, E. Pecora, and V. Zanon (2006), The exceptional activity and growth of the Southeast Crater, Mount Etna (Italy), between 1996 and 2001, *Bull. Volcanol.*, *69*, 149–173, doi:10.1007/s00445-006-0061-x.

Bonaccorso, A. (2006), Explosive activity at Mt. Etna summit craters and source modelling by using high precision continuous tilt, *J. Volcanol. Geotherm. Res.*, *158*, 221–234.

Bonaccorso, A., G. Falzone, and S. Gambino (1999), An investigation into shallow borehole tiltmeters, *Geophys. Res. Lett.*, *26*(11), 1637–1640.

Bonaccorso, A., A. Cannata, R. A. Corsaro, G. Di Grazia, S. Gambino, F. Greco, L. Miraglia, and A. Pistorio (2011a), Multi-disciplinary investigation on a lava fountain preceding a flank eruption: the 10 May 2008 Etna case, *Geochem. Geophys. Geosyst.*, *12*(7), Q07009, doi:10.1029/2010GC003480.

Bonaccorso, A., et al. (2011b), Dynamics of a lava fountain revealed by geophysical, geochemical and thermal satellite measurements: The case of the 10 April 2011 Mt Etna eruption, *Geophys. Res. Lett.*, *38*, L24307, doi:10.1029/2011GL049637.

Bonaccorso, A., S. Calvari, G. Currenti, C. Del Negro, G. Ganci, A. Linde, R. Napoli, S. Sacks, and A. Sicali (2013), From Source to Surface:

Dynamics of Etna's Lava Fountains Investigated by Continuous Strain, Magnetic, Ground and Satellite Thermal Data, *Bull. Volcanol.*, *75*, 690, doi:10.1007/500445-013-0690-9.

Calvari, S., G. G. Salerno, L. Spampinato, M. Gouhier, A. La Spina, E. Pecora, A. J. L. Harris, P. Labazuy, E. Biale, and E. Boschi (2011), An unloading foam model to constrain Etna's 11–13 January 2011 lava fountaining episode, *J. Geophys. Res.*, *116*, B11207, doi:10.1029/2011JB008407.

Comsol Multiphysics 4.3 (2012), Comsol AB, 1356 pp, Stockholm, Sweden.

Corsaro, R. A., V. Di Renzo, S. Distefano, L. Miraglia, and L. Civetta (2013), Relationship between petrologic processes in the plumbing system of Mt. Etna and the dynamics of the eastern flank from 1995 to 2005, *J. Volcanol. Geotherm. Res.*, *251*, 75–89.

Currenti, G., A. Bonaccorso, C. Del Negro, and D. Scandura (2010), Elasto-plastic modeling of volcano ground deformation, with application on Mt Etna, *Earth Planet. Sci. Lett.*, *296*, 311–318, doi:10.1016/j.epsl.2010.05.013.

Ganci, G., A. J. L. Harris, C. Del Negro, Y. Guéhenneux, A. Cappello, P. Labazuy, S. Calvari, and M. Gouhier (2012), A year of fountaining at Etna: volumes from SEVIRI, *Geophys. Res. Lett.*, *39*, L06305, doi:10.1029/2012GL051026.

Harris, A. J. L., and M. Neri (2002), Volumetric observations during paroxysmal eruptions at Mount Etna: pressurized drainage of a shallow chamber or pulsed supply?, *J. Volcanol. Geotherm. Res.*, *116*, 79–95.

Jaupart, C., and S. Vergniolle (1989), The generation and collapse of foam layer at the roof of a basaltic magma chamber, *J. Fluid Mech.*, *203*, 347–380.

Johnson, D. J., F. Sigmundsson, and P. T. Delaney (2000), Comment on "Volume of magma accumulation or withdrawal estimated from surface uplift or subsidence, with application to the 1960 collapse of Kilauea volcano" by P. T. Delaney and D. F. Mc Tigue, *Bull. Volcanol.*, *61*, 491–493.

Meertens, C. M., and J. M. Wahr (1986), Topographic effect on tilt, Strain, and displacement measurements, *J. Geophys. Res.*, *91*(B14), 14,057–14,062.

Patanè, D., P. De Gori, C. Chiarabba, and A. Bonaccorso (2003), Magma ascent and pressurization of Mt. Etna's volcanic system, *Science*, *299*, 2061–2063.

Roelloffs, E. A., and A. T. Linde (2007), Borehole observations and continuous strain and fluid pressure, in *Volcano Deformation*, pp. 305–322, Springer-Verlag, Berlin, Heidelberg, New York.

Sacks, I. S., S. Suyehiro, D. W. Evertson, and Y. Yamagishi (1971), Sacks–Evertson strainmeter, its installation in Japan and some preliminary results concerning strain steps, *Paper Meteorol. Geophys.*, *22*, 195–208.

Spera, F. (2000), Physical properties of magma, in *Encyclopedia of volcanoes*, edited by H. Sigurdsson, B. Houghton, B. McNutt, H. Rymer, and J. Stix, pp. 171–190, Academic Press, San Diego, California.

Tamura, Y., T. Sato, M. Ooe, and M. Ishiguro (1991), A procedure for tidal analysis with a Bayesian information criterion, *Geophys. J. Int.*, *104*(3), 507–516, doi:10.1111/j.1365-246X.1991.tb05697.x.

Wolff, J. A., and J. M. Sumner (2000), Lava fountains and their products, in *Encyclopedia of volcanoes*, edited by H. Sigurdsson, B. Houghton, B. McNutt, H. Rymer, and J. Stix, pp. 321–329, Academic Press, San Diego, California.